MOLECULAR AND CELLULAR BIOLOGY, July 1997, p. 3614–3628 Vol. 17, No. 7
0270-7306/97/$04.00+0
Copyright © 1997, American Society for Microbiology

Fine-Resolution Analysis of Products of Intrachromosomal Homeologous Recombination in Mammalian Cells

DI YANG† AND ALAN S. WALDMAN*

Department of Biological Sciences, University of South Carolina, Columbia, South Carolina 29208

Received 31 October 1996/Returned for modification 11 December 1996/Accepted 2 April 1997

Mouse L*tk*$^-$ cell lines that contained a herpes simplex virus type 1 (HSV-1) thymidine kinase (*tk*) gene with a 16-bp insertion mutation linked to either a defective HSV-2 *tk* gene or a hybrid *tk* sequence comprised of HSV-1 and HSV-2 *tk* sequences were constructed. HSV-1 and HSV-2 *tk* genes have 81% nucleotide identity and hence are homeologous. Correction of the insertion mutant HSV-1 *tk* gene via recombination with the hybrid *tk* sequence required an exchange between homeologous *tk* sequences, although recombination could initiate within a region of significant sequence identity. Seven cell lines containing linked HSV-1 and HSV-1–HSV-2 hybrid *tk* sequences gave rise to *tk*$^+$ segregants at an average rate of 10^{-8} events per cell division. DNA sequencing revealed that each recombinant from these lines displayed an apparent gene conversion which involved an accurate transfer of an uninterrupted block of information between homeologous *tk* sequences. Conversion tract lengths ranged from 35 to >330 bp. In contrast, cell lines containing linked HSV-1 and HSV-2 *tk* sequences with no significant stretches of sequence identity had an overall rate of homeologous recombination of $<10^{-9}$. One such cell line produced homeologous recombinants at a rate of 10^{-8}. Strikingly, all homeologous recombinants from this latter cell line were due to crossovers between the HSV-1 and HSV-2 *tk* genes. Our results, which provide the first detailed analysis of homeologous recombination within a mammalian genome, suggest that rearrangements in mammalian genomes are regulated by the degree of sequence divergence located at the site of recombination initiation.

Recombination between similar but imperfectly matched sequences is referred to as homeologous recombination. Homeologous recombination events have been recovered in several organisms, including yeast (2, 12, 15, 16, 18, 31, 32, 34, 35, 40, 43), bacteria (28, 36–39, 44, 45), and mammalian cells (3, 53). When homeologous recombination is detected, it is typically much less frequent than is recombination between highly homologous sequences. Low rates for homeologous recombination may help to conserve genomic integrity by preventing undesirable rearrangements. On the other hand, when homeologous recombination does occur, it can potentially lead to novel genes and chromosomes and may play an important role in the evolution of genomes. For these reasons, it is of considerable interest to gain knowledge about such events as they occur in a variety of organisms. We previously investigated intrachromosomal homeologous recombination between a defective herpes simplex virus type 1 (HSV-1) thymidine kinase (*tk*) sequence and a closely linked HSV-2 *tk* sequence in the genome of mouse fibroblasts (52). HSV-1 and HSV-2 *tk* sequences have 81% sequence identity, with a 35-bp stretch of sequence identity being the longest (19, 49). The rate of intrachromosomal homeologous recombination between HSV-1 and HSV-2 *tk* sequences was reduced more than 1,000-fold compared with that of intrachromosomal recombination between nearly perfectly homologous HSV-1 *tk* sequences, and we recovered no homeologous recombination events among greater than 2×10^9 cells examined in fluctuation analyses (52). Such work contributed to a body of information demonstrating that the occurrence of intrachromosomal recombination in mammalian cells is sensitive to both the percent identity and the length of sequence identity for the interacting sequences (6, 22, 41, 48, 52).

In additional efforts to study homeologous recombination (53), we designed a hybrid HSV-1–HSV-2 *tk* sequence (denoted as the donor from pHYB21-8 [see Fig. 1B]). This hybrid sequence, referred to hereafter as the hybrid donor, was used in experiments with a defective HSV-1 *tk* gene in such a manner that correction of the mutation in the HSV-1 *tk* gene required a genetic exchange with HSV-2 *tk* sequences. The adjoining segment of HSV-1 *tk* sequence on the donor provided a region of sequence identity with the defective HSV-1 *tk* gene in order to potentially enhance the recombination rate. Use of the hybrid donor allowed us to recover apparent homeologous exchanges (53).

In the current work, we employed previously used and newly designed hybrid donor sequences to expand upon prior studies by characterizing the products of putative intrachromosomal homeologous recombination events at the nucleotide level. Here we present definitive evidence for accurate exchanges of continuous blocks of information between homeologous sequences in a mammalian genome, which is consistent with gene conversions.

We additionally report a newly established cell line that permitted the study of intrachromosomal homeologous recombination between HSV-1 and HSV-2 *tk* sequences in which both initiation and resolution necessarily occurred entirely within homeologous sequences. Sequencing analysis of such "pure" homeologous recombinants revealed a striking predominance of crossovers and a complete absence of gene conversions. We present a replication-slippage model to explain these homeologous crossovers.

Our results provide the first definitive evidence for and detailed analysis of homeologous recombination within a mammalian genome and suggest that genetic rearrangements in

* Corresponding author. Mailing address: Department of Biological Sciences, University of South Carolina, Columbia, SC 29208. Phone: (803) 777-8405. Fax: (803) 777-4002. E-mail: awaldman@biol.scarolina.edu.

Present address: Section of Immunobiology, Yale University School of Medicine, New Haven, CT 06520.

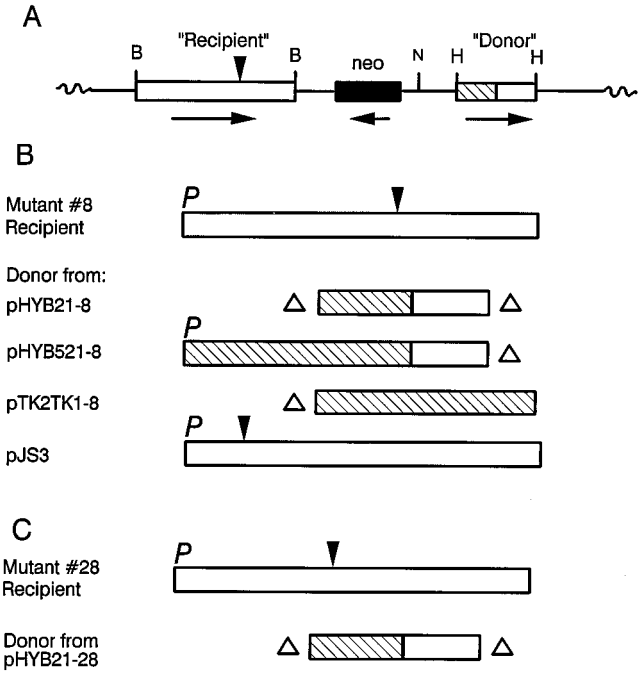

FIG. 1. Recombination substrates. (A) Illustration of a generic construct integrated into the mouse genome. Mouse genomic DNA is denoted by wavy lines flanking the construct. *Bam*HI (B), *Hin*dIII (H), and *Nde*I (N) sites are shown. Also indicated are HSV-1 *tk* (□), HSV-2 *tk* (▨), and *neo* gene (■) sequences as well as a *Xho*I linker insertion mutation (▼). The construct is depicted as having been linearized at the unique *Cla*I site in the vector prior to genomic integration. In some cell lines, the appropriate construct was linearized at the *Nde*I site prior to genomic integration (Table 1, footnote *a*). (B) Recipient *tk* gene sequence harboring *Xho*I linker mutation 8 is shown aligned in homologous register with the different donor sequences contained in constructs pHYB21-8, pHYB521-8, pTK2TK1-8, and pJS3. The truncations of *tk* coding regions on donors are indicated (△). Only the donor sequences from pHYB521-8 and pJS3 contain promoters (*P*). (C) Recipient *tk* gene sequence harboring *Xho*I linker mutation 28 is shown aligned with the donor sequence from construct pHYB21-28, which is identical to the donor sequence from pHYB21-8. See Materials and Methods for construction details.

mammals are regulated by the degree of sequence divergence at the site of initiation of recombination.

MATERIALS AND METHODS

Cell culture and derivation of experimental cell lines. Mouse L cells deficient in thymidine kinase (L*tk*$^-$ cells) were grown in Dulbecco's modified Eagle medium supplemented with 10% fetal bovine serum, 0.1 mM minimum essential medium nonessential amino acids (GIBCO, Gaithersburg, Md.), and 50 μg of gentamicin sulfate per ml. Cells were maintained at 37°C in a humidified atmosphere of 5% CO_2.

Plasmid DNA was linearized by cleavage with either *Cla*I or *Nde*I and introduced into mouse L*tk*$^-$ cells by direct microinjection (9), electroporation (26), or calcium phosphate-DNA coprecipitation (58). Stable transformants were isolated after selection in G418 (200 μg of active drug per ml) as previously described (52).

Plasmid descriptions. All the plasmids used are based on vector pJS-1, which is equivalent to pSV2neo (46) with restriction site modifications as previously described (24). The salient features of plasmids are depicted in Fig. 1. The mutant 8 HSV-1 *tk* gene (52) contains a 16-bp insertion (two 8-bp *Xho*I linkers) after nucleotide 1215 (according to the numbering of Wagner et al. [51]). The mutant 28 HSV-1 *tk* gene (52) contains an 8-bp *Xho*I linker insertion after nucleotide 1035. The mutant 26 HSV-1 *tk* gene (24) contains an 8-bp *Xho*I linker insertion after nucleotide 737. Plasmid pHYB21-8, which was called pHYB in an earlier work (53), contains the mutant 8 HSV-1 *tk* gene on a 2.5-kb *Bam*HI fragment inserted into the unique *Bam*HI site and a hybrid donor *tk* sequence inserted into the unique *Hin*dIII site of vector pJS-1. This hybrid *tk* sequence was comprised of nucleotides 848 to 1260 of the HSV-2 *tk* gene joined to nucleotides 1260 to 1621 of the HSV-1 *tk* gene. The HSV-1 and HSV-2 sequences were joined at a common *Pst*I site at position 1260 to produce a continuous, in-frame coding sequence. Plasmid pHYB521-8 is identical to pHYB21-8 except that a hybrid *tk* fragment consisting of nucleotides 262 to 1260 of the HSV-2 *tk* gene joined to nucleotides 1260 to 1621 of the HSV-1 *tk* gene is inserted at the *Hin*dIII site. This hybrid fragment contains the promoter region of the HSV-2 *tk* gene. Plasmid pHYB21-28 is identical to pHYB21-8 except that a 2.5-kb fragment containing the mutant 28 HSV-1 *tk* gene is inserted at the *Bam*HI site of the vector. Plasmid pTK2TK1-8, which has previously been described (58), contains the mutant 8 HSV-1 *tk* gene on a 2.5-kb *Bam*HI fragment inserted into the *Bam*HI site and an 800-bp *Eco*RV-*Stu*I fragment of the HSV-2 *tk* gene inserted into the *Hin*dIII site of vector pJS-1. This fragment of the HSV-2 *tk* gene is missing the 30% of the coding region that maps upstream from the *Eco*RV site as well as the polyadenylation signals downstream from the *Stu*I site. The deletion of sequences downstream from the *Stu*I site does not by itself block HSV-2 *tk* expression (52, 59). Plasmid pJS3 (24) is identical to pTK2TK1-8 except that it contains the mutant 26 HSV-1 *tk* gene on a 2.0-kb fragment inserted into the *Hin*dIII site of the vector.

Determination of intrachromosomal recombination rates. Intrachromosomal recombination rates and frequencies were determined by selecting for *tk*$^+$ segregants by hypoxanthine-aminopterin-thymidine (HAT) selection and by performing fluctuation analyses (27). For each fluctuation analysis, 10 independent subclones of a cell line were propagated to the appropriate number of cells and then plated separately into HAT medium. After a 2-week incubation, colonies were counted and rates were determined in terms of the number of events per cell generation per integrated copy of recombination substrate by solving for *a* in the formula $r = aN_t\ln(N_tCa)$, where *r* is the average number of recombinants recovered per subclone, *a* is the rate of recombination, N_t is the average number of cells per subclone at the time of selection, and *C* is the number of subclones examined (27). Rate calculations were facilitated by using the data of Capizzi and Jameson (10).

DNA preparation and Southern hybridization analysis. Genomic DNA was prepared from cultured cells and analyzed by Southern hybridization with a mixture of ^{32}P-labeled probes specific for HSV-1 and HSV-2 *tk* sequences as previously described (21). Probes for HSV-1 and HSV-2 *tk* sequences were prepared from the 2.5-kb *Bam*HI and 800-bp *Hin*dIII fragments of plasmid pTK2TK1-8, respectively.

PCR amplification and sequencing of PCR-amplified DNA. Recombinant *tk* sequences produced in lines containing DNA constructs harboring hybrid HSV-1–HSV-2 *tk* sequences were PCR amplified from genomic DNA isolated from HAT^r segregants with a pair of PCR primers, TK1A1 (5′-CCAGCGTCTTGTC ATTGGCG-3′) and TK1S1 (5′-CGGTGGGGTATCGACAGAGT-3′). The nucleotide sequence of primer TK1A1 is the sequence of the noncoding strand of the HSV-1 *tk* gene from nucleotides 308 to 327, while the sequence of primer TK1S1 is the coding sequence of the HSV-1 *tk* gene from nucleotides 1767 to 1786 (51). In some experiments involving cell lines containing pHYB521-8, primer DIY1 (5′-TGGCGTTCGTGGCCCTCATG-3′), the nucleotide sequence from positions 1078 to 1097 of the noncoding strand of the HSV-2 *tk* gene, was used in conjunction with primer TK1S1. In experiments involving cell line 8A, which contains construct pTK2TK1-8, recombinant *tk* sequences were PCR amplified from genomic DNA with a pair of PCR primers, TK1A2 (5′-TCTACAC CACACAACACCGC-3′) and TK2S1 (5′-TCGGGCTTCCGTGTTTGAAC-3′). The nucleotide sequence of primer TK1A2 is the sequence of the noncoding strand of the HSV-1 *tk* gene from nucleotides 814 to 833, while the sequence of primer TK2S1 is the coding sequence of the HSV-2 *tk* gene from nucleotides 1639 to 1662. In cells containing multiple copies of a recombination substrate, specific amplification of the recombinant *tk* sequence was facilitated by cleavage of genomic DNA with *Xho*I prior to PCR; recombinant genes were resistant to *Xho*I, whereas parental HSV-1 *tk* sequences were sensitive to *Xho*I due to the linker insertion mutation.

PCR products were ligated with *Sma*I-digested M13 phage vector (M13mp18), and DNA sequences were determined by the dideoxynucleotide chain termination method with a Sequenase version 2.0 DNA sequencing kit (U.S. Biochemicals, Cleveland, Ohio) according to the specifications of the manufacturer. Some PCR products were sequenced directly without first being cloned into an M13 vector.

RESULTS

Accurate exchange of a continuous block of information may occur between homeologous sequences within a mammalian genome. We established cell lines N3, N8, and N11, each containing one or more copies of pHYB21-8 (Fig. 1B) stably integrated into the genome of mouse L*tk*$^-$ cells. We also established cell lines HYB28C1, HYB28N2, HYB28N4, and HYB28N5, each containing one stably integrated copy of plasmid pHYB21-28 (Fig. 1C). Each of these seven cell lines contained a linker insertion mutant HSV-1 *tk* gene (either mutant 8 or 28) closely linked to a defective hybrid donor sequence. It was intended that the hybrid donor would participate in gene conversions, leading to correction of the insertion mutation in

TABLE 1. Rates of intrachromosomal homeologous recombination

DNA substrate	Cell line[a]	Copy no.[b]	No. of cells tested (10^6)	No. of HAT^r colonies	Recombination frequency[c]	Recombination rate[d]
pHYB21-8	N3	1	300	6	2.0×10^{-8}	1.4×10^{-8}
			400	0	0.0	0.0
			400	0	0.0	0.0
			377	32	8.5×10^{-8}	3.3×10^{-8}
			366	4	1.1×10^{-8}	9.1×10^{-9}
	N8	2	260	5	1.0×10^{-8}	7.2×10^{-9}
			406	1	1.2×10^{-9}	5.4×10^{-10}
			405	20	2.4×10^{-8}	1.1×10^{-8}
	N11	5	340	4	2.4×10^{-9}	1.9×10^{-9}
	Mean				1.7×10^{-8}	8.5×10^{-9}
pHYB21-28	HYB28CE1	1	333	2	6.0×10^{-9}	6.0×10^{-9}
	HYB28NE2	1	301	4	1.3×10^{-8}	1.1×10^{-8}
			353	14	4.0×10^{-8}	2.0×10^{-8}
			346	5	1.4×10^{-8}	1.0×10^{-8}
	HYB28N4	1	344	13	3.8×10^{-8}	2.0×10^{-8}
	HYB28N5	1	349	3	8.6×10^{-9}	8.2×10^{-9}
	Mean				2.0×10^{-8}	1.3×10^{-8}
pHYB521-8	HYB521NE10	1	416	908	2.1×10^{-6}	4.2×10^{-7}
			95	210	2.2×10^{-6}	5.6×10^{-7}
	HYB521NE7	1	438	182	4.2×10^{-7}	1.1×10^{-7}
	HYB521NE5	1	412	39	9.5×10^{-8}	3.5×10^{-8}
	HYB521CE5	1	465	34	7.3×10^{-8}	2.8×10^{-8}
	Mean				9.8×10^{-7}	2.3×10^{-7}
pTK2TK1-8	8A	5	310	55	3.6×10^{-8}	1.2×10^{-8}
			350	84	4.8×10^{-8}	1.4×10^{-8}
			360	26	1.4×10^{-8}	6.0×10^{-9}
	Mean				3.3×10^{-8}	1.1×10^{-8}

[a] Cell lines are grouped according to the integrated DNA substrate. Construct pHYB21-8 was linearized with *Cla*I prior to transfection to produce cell lines N3, N8, and N11; constructs pHYB21-28 and pHYB521-8 were linearized with *Cla*I to produce cell lines with C designations and with *Nde*I to produce cell lines with N designations; construct pTK2TK1-8 was linearized with *Nde*I to produce cell line 8A. All data are from independent fluctuation tests (10 subclones per fluctuation test).
[b] Number of copies of DNA construct stably integrated into the genome of each cell line, as determined by Southern blotting analysis (data not shown).
[c] Calculated by first dividing the number of HAT^r colonies obtained by the number of cells tested. This quotient was then divided by the copy number of the construct.
[d] The recombination rate is expressed in terms of the number of events per cell per generation per locus (normalized for copy number of construct).

the HSV-1 *tk* gene. As illustrated in Fig. 1, such correction required a genetic exchange between homeologous HSV-1 and HSV-2 *tk* sequences, although events could initiate within homologous sequences. In plasmid pHYB21-8 (Fig. 1B), the distance between the position of the *Xho*I linker insertion mutation on the recipient and the junction between HSV-1 and HSV-2 *tk* sequences in the hybrid donor was 45 bp, whereas in pHYB21-28 (Fig. 1C), the comparable distance was 225 bp. We have previously reported evidence (53) that homeologous exchanges could be recovered with hybrid donor *tk* sequences, whereas intrachromosomal homeologous events were not recovered when no homologous interval was provided (52). Previous Southern blotting analysis (53) provided evidence consistent with homeologous exchanges that involved hybrid donors, although the events were not analyzed at the nucleotide level and so the nature of the putative homeologous exchanges was not established in detail.

To study intrachromosomal homeologous recombination in greater depth, in the current work we isolated putative homeologous recombinants from one previously used cell line (N3) and six newly established cell lines (N8, N11, HYB28C1, HYB28N2, HYB28N4, HYB28N5) and analyzed the products of homeologous recombination at the nucleotide level. As indicated in Table 1, each of the seven cell lines containing pHYB21-8 or pHYB21-28 gave rise to HAT^r segregants. The average recombination rate (normalized to the number of copies of the integrated construct) for cell lines containing pHYB21-8, 8.5×10^{-9} (Table 1), was not very different from the recombination rate for cell lines containing pHYB21-28, 1.3×10^{-8}. The rates involving hybrid donors were about 10-fold lower than those obtained in experiments with an HSV-1 *tk* genetic donor of comparable length and having perfect homology with an insertion mutant HSV-1 *tk* gene (53, 59).

Because the donor sequences on pHYB21-8 and pHYB21-28 had 5′ and 3′ deletions of coding sequences (Fig. 1B and 1C), only gene conversions or double crossovers were recoverable from these recombination substrates; single crossovers would have produced nonfunctional *tk* genes with 5′ or 3′ truncations. Genomic DNAs were isolated from several HAT^r segregants and subjected to Southern blotting analysis to obtain evidence that a gene conversion had occurred in each HAT^r segregant. A representative analysis of parental cell line N8 and a HAT^r segregant from cell line N8 is presented in Fig. 2. The configuration of integrated copies of pHYB21-8 in parental cell line N8 as well as the expected structure for a recombinant are illustrated schematically in Fig. 3. Parental cell line N8 contains two copies of pHYB21-8 integrated in a tandem array. When genomic DNA from cell line N8 was digested with *Bam*HI and probed with a *tk*-specific probe (Fig. 2, panel 1, left lane), bands of 6.5 and 2.5 kb were visible along with a junction fragment as expected (compare with Fig. 3). When DNA from cell line N8 was digested with *Bam*HI plus *Xho*I (Fig. 2, panel 1, right lane), the 2.5-kb *Bam*HI fragments

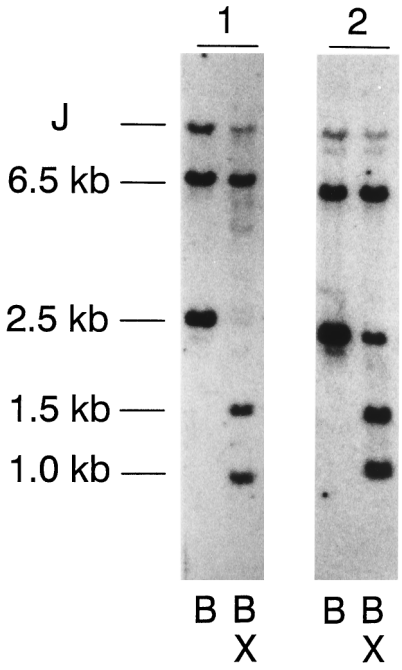

FIG. 2. Southern blotting analysis of cell line N8 and a representative HAT^r recombinant. Genomic DNA (8-μg) samples from cell line N8 (panel 1) and a HAT^r segregant (panel 2) were digested with *Bam*HI (B) or *Bam*HI plus *Xho*I (BX) and subjected to Southern blotting analysis with a *tk*-specific probe as described in Materials and Methods. The pattern of hybridizing bands for the HAT^r segregant is consistent with a gene conversion (Fig. 3) (see text for further discussion). J, junction fragment.

were cleaved with *Xho*I into the predicted 1.5- and 1.0-kb bands. In contrast, digestion of DNA from a HAT^r segregant with *Bam*HI or *Bam*HI plus *Xho*I (Fig. 2, panel 2) indicated that one of the 2.5-kb *Bam*HI fragments was cleavable with *Xho*I but that the other resisted cleavage. This was the pattern expected for a cell in which a homeologous gene conversion had eliminated the *Xho*I linker insertion mutation in one of the two mutant HSV-1 *tk* genes (Fig. 3).

Recombinant *tk* sequences were PCR amplified from the genomes of several HAT^r segregants in which Southern blotting analysis suggested that a homeologous gene conversion had occurred, and sequence analysis was performed. (The positions of the PCR primers used are indicated schematically above the recombinant *tk* gene in Fig. 3.) For each of 12 HAT^r segregants from cell lines containing pHYB21-8 and 3 HAT^r segregants from cell lines containing pHYB21-28, a sequence of 1,479 bp, spanning nucleotides 308 to 1786 of the *tk* coding region, was determined. Because of the numerous differences between the HSV-1 and HSV-2 *tk* sequences, the parental origins of many of the nucleotides in recombinant sequences were assignable unambiguously. The results of this sequence analysis are summarized in Table 2 and are depicted schematically in Fig. 4. The actual nucleotide sequences of the pertinent regions of the HSV-1 and HSV-2 *tk* genes are presented in Fig. 5.

Each HAT^r segregant analyzed had undergone an accurate transfer of a continuous block of information from the HSV-2 *tk* sequence to the HSV-1 insertion mutant *tk* gene. The *Xho*I linker insertion was corrected in all cases. The lengths of conversion tracts varied from at least 35 to >331 bp (Table 2). Further analysis is provided below (see Discussion).

In cell lines containing pHYB21-8 or pHYB21-28, only homeologous gene conversions (or double crossovers) could be recovered as discussed above. These cell lines were designed with the knowledge that >80% of all homologous recombination events in our experimental system were previously found to be consistent with gene conversions (5, 6, 20, 24, 54). To gain a more complete understanding of the nature of homeologous exchanges, we established cell lines HYB521NE10, HYB521 NE7, HYB521NE5, and HYB521CE5, each of which contained a single integrated copy of plasmid pHYB521-8 (Fig. 1B). The average rate of formation of HAT^r segregants from cell lines containing pHYB521-8 was 2.3×10^{-7} (Table 1).

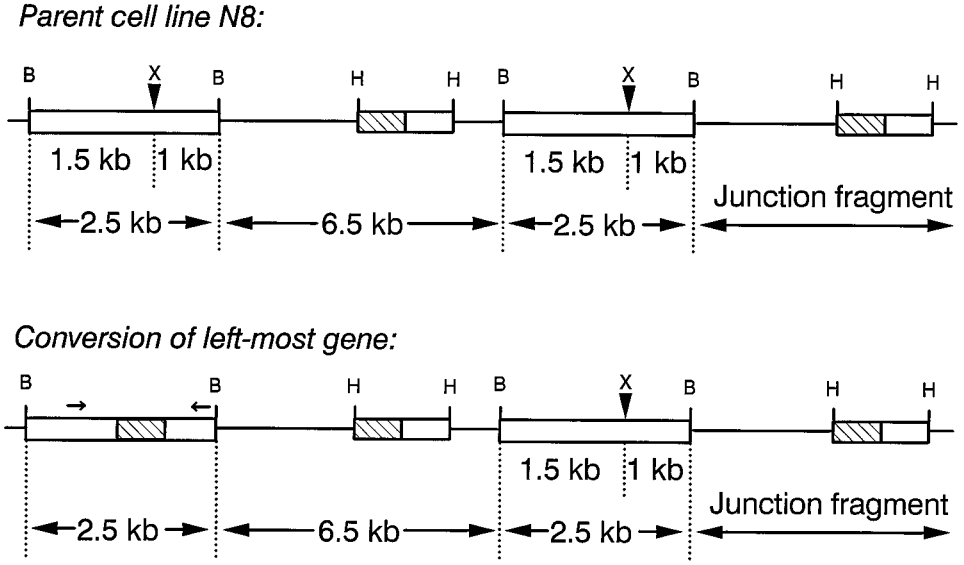

FIG. 3. Structures of an integrated tandem duplication of construct pHYB21-8 in cell line N8 and a HAT^r segregant arising from a gene conversion. The symbols are the same as those described in the legend to Fig. 1. *Bam*HI (B), *Hin*dIII (H), and *Xho*I (X) sites are indicated. These schematic diagrams depict the origins of the *Bam*HI and *Bam*HI/*Xho*I digestion products visualized in the Southern blot of Fig. 2. The rough positions of PCR primers used to amplify sequences from recombinants for subsequent sequencing analysis are indicated by small arrows above the recombinant *tk* sequence. Conversion of the rightmost gene is also possible.

TABLE 2. Analysis of intrachromosomal homeologous gene conversions that involved hybrid HSV-1–HSV-2 *tk* donor sequences

Cell line and recombinant(s)[a]	Tract end[b]		Minimum tract length (bp)[c]	Boundary of tract ends (bp)[d]
	5′	3′		
Containing pHYB521-8				
N22, N241, N8-6	921–929	ND	331	9
N242	1151–1154	ND	106	4
N293, N3-3-4, N3-4, N3-6-1	1157–1170	ND	90	14
N3, N3-4a, N8-1, N8-6-1	1172–1177	ND	83	6
Containing pHYB21-28				
N27, N28	1011–1016	ND	244	6
28N4	1018–1021	1055–1076	35	4 (21)
Containing pHYB521-8				
2a, 4a, 10a	1185–1204	ND	56	20
7a	1206–1211	ND	49	6

[a] Independent recombinants are grouped according to the parental cell lines from which they arose as well as by conversion tract lengths, as determined by sequencing. The names used to denote various recombinants are the same as those in Fig. 4. The independence of recombinants was ensured by taking recombinants from different subcultures.

[b] Conversion tract ends were mapped as accurately as possible by using nucleotide heterologies between HSV-2 donor and HSV-1 recipient *tk* sequences (Fig. 5). Most 3′ tract ends mapped within the region of perfect homology between donor and recipient *tk* sequences and thus could not be determined precisely (ND).

[c] Minimum length of HSV-2 *tk* sequence within each conversion tract.

[d] Length of the segment of identity between HSV-1 and HSV-2 *tk* sequences within which the 5′ end of each conversion tract mapped. Only recombinant 28N4 (from a cell line containing pHYB21-28) had a mappable 3′ conversion tract end, and the boundary of this 3′ end is presented in parentheses.

Twenty-eight independent HAT^r clones from cell lines containing pHYB521-8 were screened by Southern blotting with a probe specific for HSV-1 *tk* sequences. A representative Southern blotting analysis for three recombinants is presented in Fig. 6, and the origins of the fragments visualized on the blot are depicted in Fig. 7. Because the hybrid *tk* sequence on pHYB521-8 contained the promoter for the HSV-2 *tk* gene, single crossovers as well as gene conversions were theoretically recoverable. However, since the hybrid *tk* sequence had a 3′ truncation, any functional *tk* gene produced by a crossover would have to utilize the HSV-2 *tk* promoter and the crossover site would have to occur downstream from the position of the *Xho*I linker insertion in the HSV-1 *tk* gene (Fig. 1B). The DNA segment within which a productive crossover could occur consisted of a 45-bp region of homeology immediately downstream from the insertion mutation and a 360-bp interval of sequence identity downstream from the homeologous sequences.

For cell lines HYB521NE10, HYB521NE7, and HYB521NE5, in which pHYB521-8 had been linearized at the *Nde*I site prior to integration (Fig. 7), the hybrid donor was positioned upstream from the insertion mutant *tk* gene; hence, both intrachromatid and unequal sister chromatid crossovers were recoverable. Either type of crossover would produce a single diagnostic 1.5-kb *Bam*HI fragment resistant to *Xho*I cleavage (Fig. 7). Eight of 10 recombinants from HYB521NE7 and 8 of 10 recombinants from HYB521NE10 exhibited this pattern of DNA fragments. An example of such a recombinant is displayed in Fig. 6, lanes 1 and 2. Gene conversions were also recoverable, and in such cases, genetic exchange would have had to occur between homeologous sequences in order to correct the linker insertion (Fig. 1B). A gene conversion would produce a diagnostic 2.5-kb *Bam*HI fragment resistant to cleavage by *Xho*I, as well as a 2.3-kb *Bam*HI fragment (Fig. 7). Two recombinants from HYB521NE7 and two from HYB521NE10 exhibited this pattern, and an example is displayed in Fig. 6, lanes 3 and 4. For cell line HYB521CE5, in which pHYB521-8 had been linearized at the *Cla*I site (Fig. 7), unequal sister chromatid crossovers were recoverable but intrachromatid crossovers were not recoverable because the 3′-truncated hybrid *tk* sequence was positioned downstream from the insertion mutant HSV-1 *tk* gene. An unequal sister chromatid crossover would produce a triplication of *tk* sequences (Fig. 7) containing a 1.5-kb *Bam*HI fragment as well as a 2.5-kb *Bam*HI fragment and a junction fragment. The 2.5-kb *Bam*HI fragment would retain the linker insertion and thus be cleavable by *Xho*I into 1.5- and 1.0-kb fragments. All eight recombinants from cell line HYB521CE5 that were analyzed exhibited this pattern, and an example is displayed in Fig. 6, lanes 5 and 6. (Gene conversions were also potentially recoverable from cell line HYB521CE5, although none were recovered among the eight recombinants analyzed.)

In summary, of 28 recombinants analyzed from cell lines containing pHYB521-8, 24 (86%) displayed patterns consistent with crossovers and 4 (14%) displayed patterns consistent with homeologous gene conversions. The rate of recovery of homeologous gene conversions ($14\% \text{ of } 2.3 \times 10^{-7} = 3.2 \times 10^{-8}$) was similar to or perhaps slightly greater than that recorded for cell lines containing pHYB521-8 or pHYB21-28 (Table 1).

Reconstructed *tk* genes were PCR amplified from the genomes of HAT^r segregants of cell lines containing pHYB521-8 and were sequenced. For crossover recombinants, all crossover points were located within the region of sequence identity between the insertion mutant HSV-1 and hybrid *tk* sequences and therefore could not be mapped precisely. The observation that 24 of 28 recovered events did not display a recombination junction within the homeologous interval suggested that most events both initiated and resolved within the region of sequence identity.

Sequencing analysis confirmed that 4 of 28 clones (recombinants 2a, 4a, 7a, and 10a) (Fig. 4A; Table 2) had undergone a gene conversion that encompassed homeologous sequences. The four gene conversion tracts were accurate, uninterrupted, and between 49 and 56 bp in length.

Intrachromosomal recombination events initiating within homeologous sequences result in crossovers. We reported that the rate of intrachromosomal recombination between closely linked HSV-1 and HSV-2 *tk* genes is $<4 \times 10^{-10}$; indeed, no such events were recovered previously (52). In a renewed attempt to recover such recombinants, we established several additional cell lines containing pTK2TK1-8 (Fig. 1B). One such cell line, 8A, was estimated to contain five copies of pTK2TK1-8 integrated at three distinct loci; two of the integration sites were each judged to contain a tandem duplication

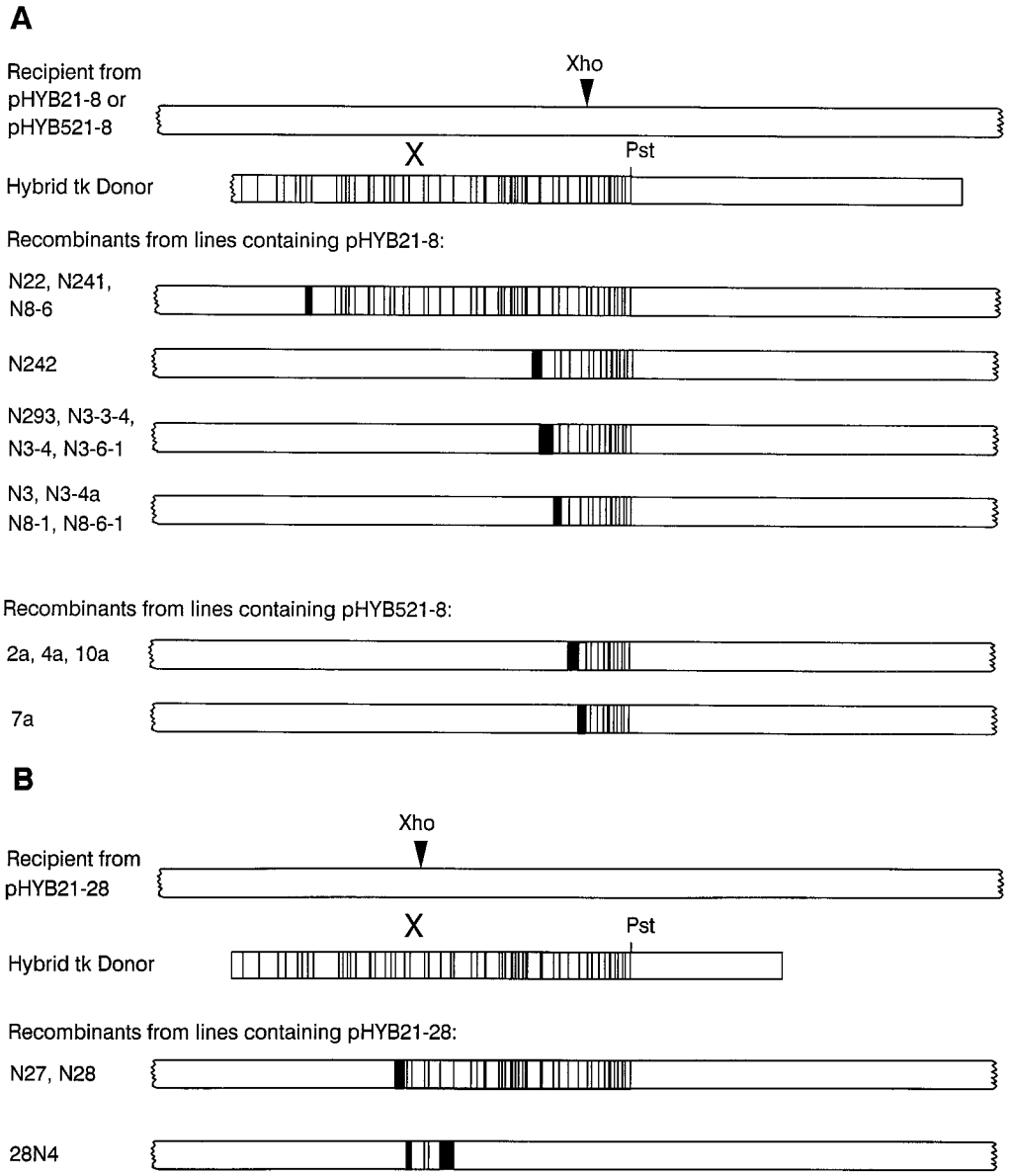

FIG. 4. Gene conversion tracts produced by intrachromosomal homeologous recombination between insertion mutant HSV-1 *tk* genes and hybrid *tk* donors. HSV-1 *tk* sequences are represented by open rectangles, and nucleotide differences between HSV-1 and HSV-2 *tk* gene sequences are represented by vertical black lines. Darkened regions at the ends of conversion tracts represent intervals of identity between HSV-1 and HSV-2 *tk* sequences within which the terminus of each conversion tract maps. The names of recombinants are the same as those in Table 2. Shown are conversion tracts correcting the mutant 8 (A) and 28 (B) HSV-1 *tk* genes.

of pTK2TK1-8 (data not shown). Cell line 8A gave rise to HAT^r segregants at a rate of 1.1×10^{-8} (Table 1). Cell line 8A provided a unique opportunity to examine the products of intrachromosomal recombination events with obligatory initiation and resolution sites within homeologous sequences in the absence of any significant length of sequence identity.

The HSV-2 *tk* sequence in pTK2TK1-8 was truncated at the 5′ end but extended to the 3′ end of the coding region (Fig. 1B). Therefore, HAT^r segregants arising in cultures of cell line 8A could in principle have resulted from either a crossover between the HSV-1 and HSV-2 *tk* gene or a gene conversion in which the linker insertion (mutation 8) in the HSV-1 *tk* gene had been corrected. Because of the 5′ truncation of the HSV-2 *tk* sequence, any crossover producing a functional *tk* gene in 8A would have to occur upstream from the *Xho*I linker insertion mutation and the functional *tk* gene would utilize the HSV-1 *tk* promoter (Fig. 1B).

DNA samples isolated from 27 independent HAT^r segregants from cell line 8A were analyzed by Southern hybridization. A representative analysis of a HAT^r segregant from cell line 8A is presented in Fig. 8. An illustration of a genomic locus of cell line 8A containing an integrated tandem duplication of pTK2TK1-8 and an illustration of the expected structure for a crossover recombinant are presented in Fig. 9.

After digestion with *Bam*HI, *Hin*dIII, *Bam*HI plus *Hin*dIII, or *Bam*HI plus *Hin*dIII and *Xho*I, 7 of the 27 HAT^r segregants analyzed displayed a pattern of bands identical to that displayed by parental cell line 8A (Fig. 8, lanes 1 through 4). These HAT^r segregants, each of which likely arose via the introduction of a mutation within the HSV-1 *tk* gene that

FIG. 5. HSV-1 and HSV-2 *tk* nucleotide sequences. Shown are *tk* gene sequences from the 5′ end of the HSV-2 *tk* sequence in pHYB521-8, pHYB21-28, or pTK2TK1-8 to the *Pst*I site common to HSV-1 and HSV-2 *tk* genes. This *Pst*I site marks the 3′ end of the HSV-2 *tk* portion of the hybrid donor sequence in pHYB521-8, pHYB21-28, or pHYB521-8. Also indicated are the positions of *Xho*I linker insertion mutations 8 and 28 (open triangles) in the HSV-1 *tk* gene. Identical nucleotides in the HSV-1 and HSV-2 *tk* sequences are indicated by asterisks in the HSV-2 sequence.

compensated for the linker insertion mutation, were not analyzed further. The remaining 20 HAT^r segregants produced hybridization patterns like that of the recombinant shown in lanes 5 through 8 of Fig. 8. Digestion with either *Bam*HI or *Hin*dIII (Fig. 8, lanes 5 and 6) produced a 3.4-kb band that was not present in the parental cell line (Fig. 8, lanes 1 and 2). As illustrated in Fig. 9, a crossover recombinant was expected to produce these novel 3.4-kb bands. Upon simultaneous digestion with *Bam*HI and *Hin*dIII (Fig. 8, lane 7), a 2.0-kb band that was not present in the *Bam*HI-*Hin*dIII double digest of the parental cell line (lane 3) was displayed. The absence of this 2.0-kb band after digestion with either *Bam*HI (Fig. 8, lane 5) or *Hin*dIII (lane 6) alone demonstrated that this 2.0-kb DNA fragment terminated at a *Bam*HI site at one end and a *Hin*dIII site at the other end. Further, this 2.0-kb *Bam*HI/*Hin*dIII fragment was resistant to cleavage by *Xho*I digestion (Fig. 8, lane 8). We therefore inferred that this novel 2.0-kb fragment was the 2.0-kb *Bam*HI/*Hin*dIII fragment diagnostic for a homeologous crossover (Fig. 9). Additional copies of the 0.8-kb *Hin*dIII and 2.5-kb *Bam*HI fragments originating from the remaining unrearranged integrated copies of pTK2TK1-8 were displayed (Fig. 8, lane 7). The unrearranged copies of the 2.5-kb *Bam*HI fragment were cut with *Xho*I into 1.5- and 1-kb fragments (Fig. 8, lane 8), as were the 2.5-kb *Bam*HI fragments in the parent DNA (Fig. 8, lane 4), as expected (Fig. 9). In Fig. 8, lanes 9 through 11, *Hin*dIII digests of DNA samples isolated from three additional recombinants are displayed. As shown, the intensities of the 8.3- and 0.8-kb *Hin*dIII fragments (Fig. 9 shows the origins of these fragments) varied among the recombinants analyzed, suggesting that a tandem array of integrated copies of pTK2TK1-8 had been expanded in some recombinants but not in others. This in turn indicated that recombination did not occur between the very same two *tk* sequences in all recombinants. Additional bands visible in *Bam*HI or *Hin*dIII digests (Fig. 8, lanes 1, 2, 5, 6, and 9 through 11) represent junction fragments for the multiple sites of integration of construct pTK2TK1-8.

A striking feature of these recombinants revealed by Southern blotting analysis was that none of the 27 HAT^r segregants analyzed displayed a hybridization pattern consistent with gene conversion. Such a clone would have produced a 2.5-kb *Bam*HI fragment resistant to *Xho*I cleavage.

Recombinant hybrid *tk* genes from 19 independent HAT^r segregants arising from cell line 8A were PCR amplified for subsequent DNA sequence analysis. Based on the Southern blotting analysis described above, we inferred that these putative recombinants arose from a single crossover between HSV-1 and HSV-2 *tk* sequences. We expected such crossover products to have a promoter and 5′ region composed of HSV-1 *tk* sequences since the HSV-2 *tk* sequence on pTK2TK1-8 lacked a promoter. This allowed the expedient use of PCR primers in which the upstream primer was specific for HSV-1 *tk* sequence and the downstream primer was specific for HSV-2 *tk* sequence (Fig. 9). For each recombinant amplified,

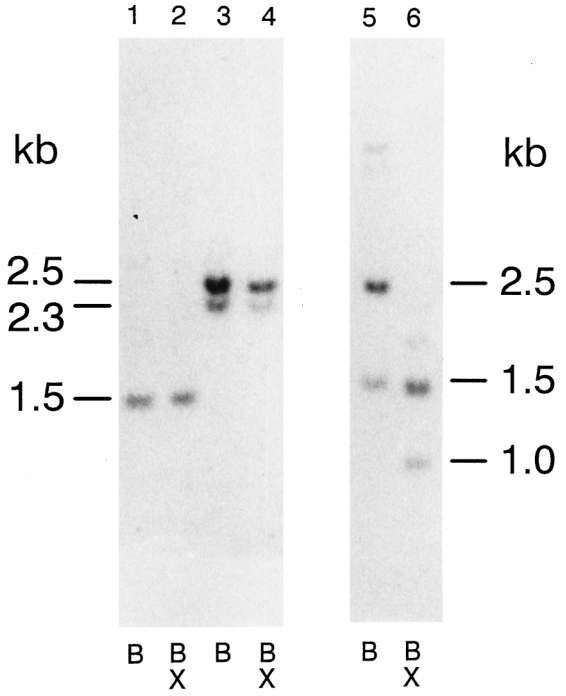

FIG. 6. Southern blotting analysis of representative HAT^r recombinants from cell lines containing pHYB521-8. Genomic DNA (8-μg) samples from HAT^r segregants isolated from cell lines containing an integrated copy of pHYB521-8 were digested with *Bam*HI (B) or *Bam*HI plus *Xho*I (BX) and displayed in pairs of lanes on a Southern blot. The probe used was specific for HSV-1 *tk* sequences; therefore, *Bam*HI fragments containing HSV-2 *tk* but lacking HSV-1 *tk* sequences were not detected. The origins of visualized bands are depicted in Fig. 7. The recombinants displayed in lanes 1 through 4 are from cell lines containing pHYB521-8 linearized with *Nde*I prior to genomic integration (Fig. 7). The recombinant in lanes 1 and 2 arose from either an intrachromatid or an unequal sister chromatid crossover (16 recombinants displayed this pattern). The recombinant in lanes 3 and 4 arose from gene conversion of the insertion mutant HSV-1 *tk* gene (four recombinants displayed this pattern). The recombinant in lanes 5 and 6 is from a cell line containing pHYB521-8 linearized with *Cla*I (Fig. 7) and arose from an unequal sister chromatid crossover (eight recombinants displayed this pattern). The faint bands in lanes 5 and 6 are junction fragments (Fig. 7). See text for further details.

a sequence of 849 bp, spanning the *tk* sequence from nucleotide positions 814 to 1662, was determined. The results of this sequence analysis are summarized in Table 3 and Fig. 10.

Among the 19 recombinant *tk* sequences studied, only one nucleotide that did not match either the HSV-1 or HSV-2 parental sequence was found. (We ascertained that this mutation was not a PCR artifact by repeating the PCR and sequencing several independently cloned PCR products.) This A-to-C transversion mutation at position 1504 appeared in recombinant 8A-35 (Table 3). Both HSV-1 and HSV-2 sequences have an A at this position. This transversion leads to a substitution of alanine for aspartic acid in the protein.

In all cases, recombinant junctions were found to correspond to an accurate in-frame joining between homeologous parental HSV-1 and HSV-2 *tk* sequences (as might be expected since selection for *tk* function would have likely precluded the recovery of grossly inaccurate or out-of-frame recombinant junctions). All recombinant hybrid *tk* sequences displayed a unique crossover point without interspersion of short patches of HSV-1 and HSV-2 *tk* sequences. The positions of the crossover points in the 19 recombinants studied are represented in Fig. 10 and are listed in Table 3. Crossover sites did not correspond to the longest stretches of sequence identity (Table 3) but did display a conspicuous degree of clustering. Eleven of 19 crossover sites were situated within 11 bp upstream of the 16-bp *Xho*I linker insertion mutation in the HSV-1 *tk* gene (Fig. 10; Table 3). The results for cell line 8A were markedly different from the types of recombination events previously observed for intrachromosomal homologous recombination (5, 6, 20, 24, 54), as well as the homeologous exchanges involving hybrid donor sequences described above, in which gene conversions were recovered.

Because the absence of gene conversions from the set of homeologous recombinants from cell line 8A represented so striking a difference from the types of events recovered when substantial homology was present, we decided to generate three new cell lines containing pJS3 (Fig. 1B) in order to more directly compare intrachromosomal homeologous recombination and intrachromosomal homologous recombination. Each of two cell lines, JS36 and JS37, contained a single integrated copy of pJS3, and cell line JS38 contained an estimated six copies of pJS3, two of which appeared to be arranged as a tandem duplication (data not shown). For each cell line, pJS3 had been linearized with *Nde*I prior to integration. Fluctuation tests with cell lines JS36, JS37, and JS38 revealed homologous recombination rates of 6.0×10^{-6}, 4.5×10^{-6}, and 4.4×10^{-6}, respectively (rates normalized to copy number).

A Southern blotting analysis of representative recombinants from cell line JS37 is shown in Fig. 11. A schematic diagram of the recombination substrate in cell line JS37 and the structures of three possible types of recombinants are provided in Fig. 12. In cell line JS36 or JS37, a functional *tk* gene could theoretically be produced by conversion of either of the two *tk* genes by using the other gene as a genetic donor or, alternatively, by an unequal sister chromatid crossover. (An intrachromatid crossover would result in a pop out of the functional *tk* gene which would not likely be recovered.) All three types of recombination events illustrated in Fig. 12 were indeed recovered. A gene conversion of the rightmost *tk* gene flanked by *Bam*HI sites is displayed in Fig. 11, lanes 3 and 4. In this recombinant, the 2.5-kb *Bam*HI fragment was resistant to cleavage by *Xho*I, whereas in the parental cell line this fragment was susceptible to *Xho*I cleavage (Fig. 11, lanes 1 and 2). A gene conversion of the leftmost *tk* gene flanked by *Hin*dIII sites in which the 2.0-kb *Hin*dIII fragment gains resistance to *Xho*I cleavage is displayed in Fig. 11, lanes 7 and 8. Finally, the expected pattern for an unequal sister chromatid crossover which produces a triplication of *tk* sequences (Fig. 12) is displayed in Fig. 11, lanes 5 and 6. Of note is the increased intensity of the 2.5-kb band in the *Bam*HI/*Hin*dIII digest (Fig. 11, lane 5), as well as the production of 1.5-, 1.0-, and 0.5-kb bands upon the addition of *Xho*I (Fig. 11, lane 6). One copy of the 2.5-kb band in the *Bam*HI/*Hin*dIII digest resisted cleavage with *Xho*I (Fig. 11, lane 6). Of the 48 HAT^r segregants from cell lines JS36, JS37, and JS38 analyzed, 39 (81%) were found to be gene conversions and the balance consisted of crossovers.

DISCUSSION

Here, we present the first direct evidence that accurate genetic exchanges can occur within a mammalian genome between two DNA sequences with as little as 81% sequence identity. An examination of the nucleotide sequences of recombinant *tk* genes isolated from 19 HAT^r segregants arising from cell lines containing pHYB521-8, pHYB21-28, or pHYB521-8 (Fig. 4; Table 2) revealed that an accurate transfer of information had indeed occurred between the homeologous HSV-1 and HSV-2 *tk* sequences in each case. Each gene conversion tract was mutation free. Similar accuracy in recombi-

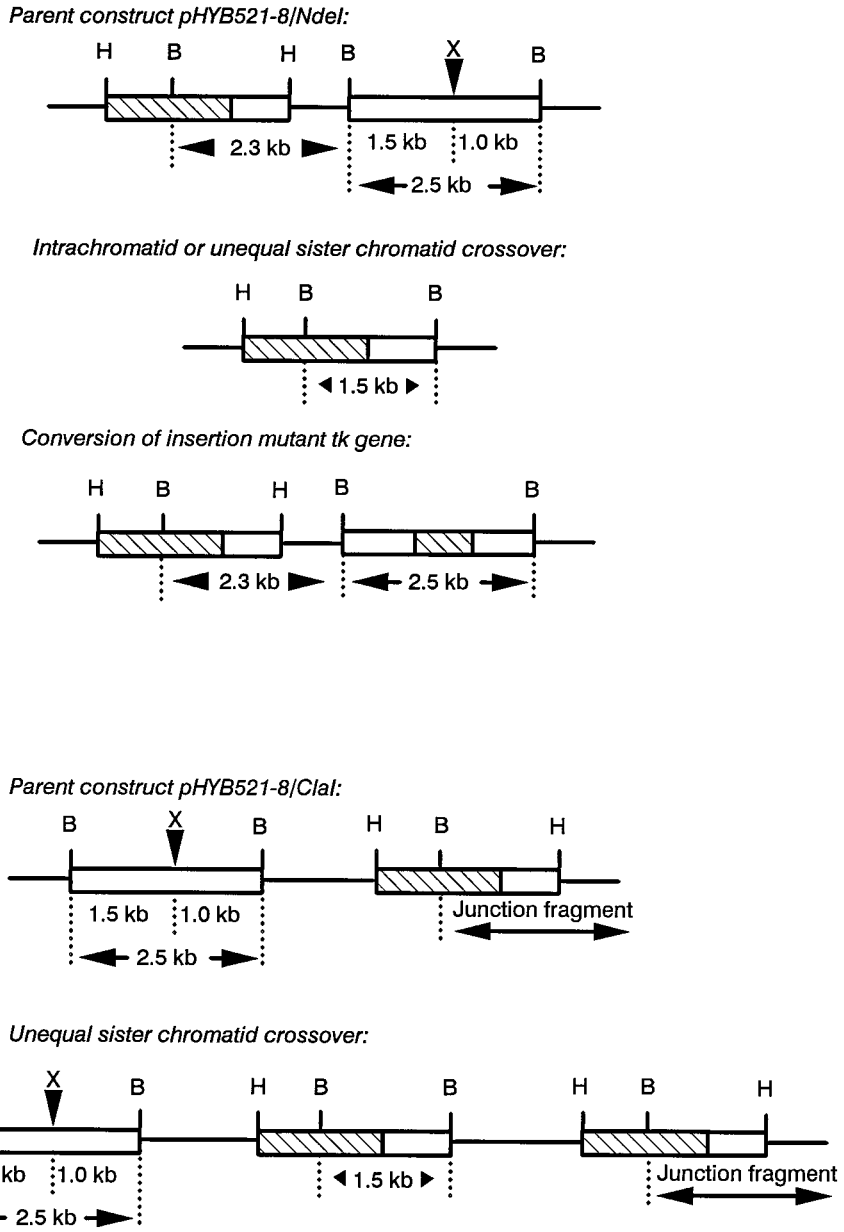

FIG. 7. Structures of three types of recombinants recovered from cell lines containing an integrated copy of pHYB521-8 linearized at the unique *Nde*I (top) or *Cla*I (bottom) site. The symbols are the same as those described in the legend to Fig. 1. The direction of transcription of the *tk* genes is from left to right. In the parental constructs, the hybrid *tk* sequence flanked by *Hin*dIII sites has a promoter but is defective due to a 3′ truncation of coding sequence. The lengths of the *Bam*HI restriction fragments diagnostic for the different types of recombination events are indicated. The indicated *Bam*HI fragments were visualized by Southern blotting analysis with a probe specific for HSV-1 *tk* sequences (Fig. 6). For the unequal sister chromatid crossover leading to a *tk* sequence triplication, the functional *tk* gene is in the middle.

nation has been reported for homeologous recombination in yeast (18, 32) and for homologous recombination in mammalian cells (47), although evidence for mutagenic homeologous recombination in yeast has also previously been presented (56). We found a single mutation in 1 of 19 crossover recombinants from a cell line, 8A, containing pTK2TK1-8. A limitation to our assessment of the accuracy of homeologous recombination, and our experimental determinations in general, is that selection for *tk* function in our experiments would likely have precluded the recovery of certain events. Nonetheless, our results illustrate that 81% sequence identity is sufficient to support accurate genetic exchanges within a mammalian genome.

Using sequences with many fewer markers to differentiate between parental sequences, others have presented evidence consistent with the hypothesis that intrachromosomal homologous recombination in mouse cells involves a transfer of a continuous block of information (23). In our experimental scheme, the multitude of silent genetic markers provided an exceptional opportunity to construct fine-resolution maps of recombination products. We determined that all conversion tracts analyzed were indeed continuous (Fig. 4). Continuous

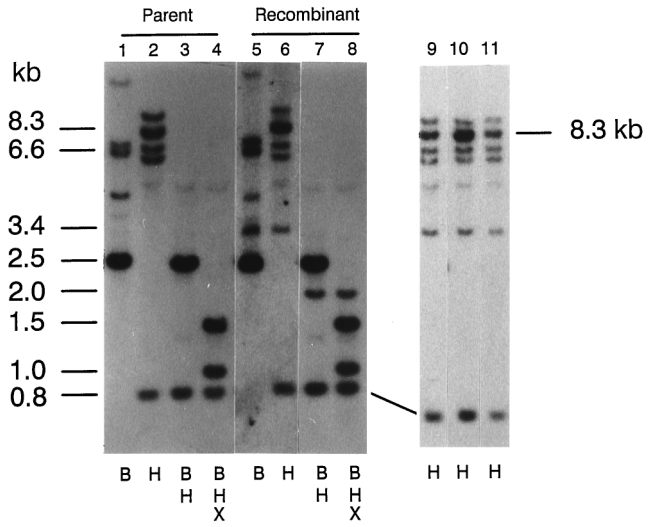

FIG. 8. Southern blotting analysis of cell line 8A and representative HAT^r recombinants. Genomic DNA (8-μg) samples from parental cell line 8A (lanes 1 through 4) and a HAT^r segregant (lanes 5 through 8) were digested with *Bam*HI (B), *Hin*dIII (H), *Bam*HI plus *Hin*dIII (BH), or *Bam*HI plus *Hin*dIII and *Xho*I (BHX) and displayed on a Southern blot with a *tk*-specific probe. The pattern of hybridizing bands for the HAT^r segregant is consistent with that expected for a homeologous crossover (Fig. 9) (see text for further discussion). *Hin*dIII digests of DNA samples from three additional recombinants (lanes 9 through 11) are also presented.

conversion tracts have also been reported for recombination in yeast (15, 18, 31–34) and bacteria (28). There have been a few reports of patchy conversion tracts for recombination in yeast (16) and mammalian cells (7, 13), although the latter two studies did not involve intrachromosomal events. A continuous conversion tract could be produced by a heteroduplex DNA (hDNA) intermediate (30) that is repaired as a continuous span by using a single template or remains unrepaired and is

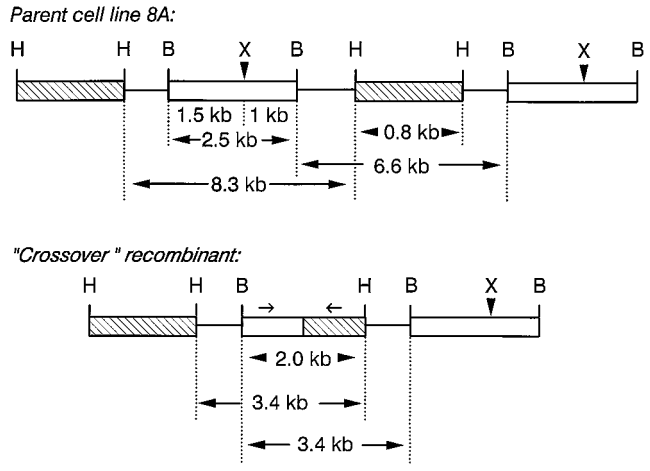

FIG. 9. Structures of an integrated tandem duplication of construct pTK2TK1-8 in cell line 8A and a HAT^r segregant arising from a crossover between homeologous sequences. The symbols are the same as those described in the legend to Fig. 1. Indicated are the origins of the expected fragments generated by digestion with *Bam*HI (B), *Hin*dIII (H), and *Xho*I (X) in various combinations and visualized on the Southern blot of Fig. 8. The crossover recombinant could arise via an intrachromatid exchange or an unequal exchange between sister chromatids. The rough positions of PCR primers used to amplify sequences from recombinants for subsequent sequencing analysis are indicated by small arrows above the recombinant *tk* sequence.

TABLE 3. Analysis of intrachromosomal homeologous crossovers produced in cell line 8A

Recombinant(s)[a]	Crossover point[b]	Distance from *Xho*I site[c]	Boundary of crossover junction[d]
8A-32	1217	0	4
8A-1, -7, -18, -33, -49	1212	4	6
8A-3, -5, -39, -43, -47	1205	11	20
8A-4, 8A-19	1178	38	6
8A-9, 8A-11	1171	45	14
8A-16	1097	119	19
8A-2	1077	139	21
8A-35	900	316	18
8A-12	863	353	17

[a] Recombinant hybrid *tk* genes from 19 independent HAT^r segregants arising from cell line 8A were sequenced. The names of recombinants are the same as those in Fig. 10.

[b] Defined as the position of the first base pair at the 5′ end of the HSV-2 *tk* portion of the recombinant hybrid HSV-1–HSV-2 *tk* gene.

[c] Number of base pairs from the crossover site to the position of the *Xho*I linker insertion in the mutant 8 HSV-1 *tk* gene.

[d] Number of base pairs of contiguous homology between the HSV-1 and HSV-2 *tk* sequences mapping immediately upstream from the crossover site (Fig. 5).

restored to homoduplex by replication. Evidence for the involvement of hDNA repair during intrachromosomal homologous recombination in mammalian cells (4) and yeast (reviewed in reference 33) has been reported. Continuous conversion tracts could also be the product of a double-strand break repair mechanism, as originally proposed for yeast (50). Greater elucidation of the pathways and intermediates involved in homeologous recombination in mammalian genomes will require further investigation.

There is some evidence that in yeast, homeologous gene conversion tracts are shorter than are homologous gene conversion tracts (18). In our current experiments involving hybrid donor cell lines, the lengths of homeologous conversion tracts ranged from 35 to 331 bp (Table 2). It may be inferred from previous studies that the lengths of homologous conversion tracts in mouse cells are often <200 bp (23); therefore, we cannot conclude that homeologous tracts are shorter. If homeologous recombination indeed proceeds via an hDNA intermediate, our data suggest that homeology does not effectively block branch migration (at least when hybrid donors are used).

We could not explicitly distinguish the beginning from the end of a conversion tract; therefore, it remains a formal possibility that in experiments with hybrid donors, gene conversions actually initiated within homeologous sequences and resolved within homologous sequences. In this scenario, resolution has a greater requirement for homology than does initiation and the homologous portion of the hybrid donor enhanced the recombination rate (relative to that of a purely homeologous cross) by providing a suitable site for resolution. The latter hypothesis may be viewed as problematic, however. If initiation and resolution are temporally distinct phases of recombination, then at the outset of recombination between homeologous sequences a cell would not know whether sufficient homology exists to ultimately allow resolution. Therefore, in order for intrachromosomal homeologous recombination to be prevented, a cellular mechanism would have to exist to completely reverse any hDNA formed once it was determined that no suitable resolution site exists. Another possibility is that the initiation of recombination in the absence of a length of homology needed for resolution leads to cell death. We prefer what seems to be a simpler scenario in which a particularly high degree of sequence identity is needed in order for recom-

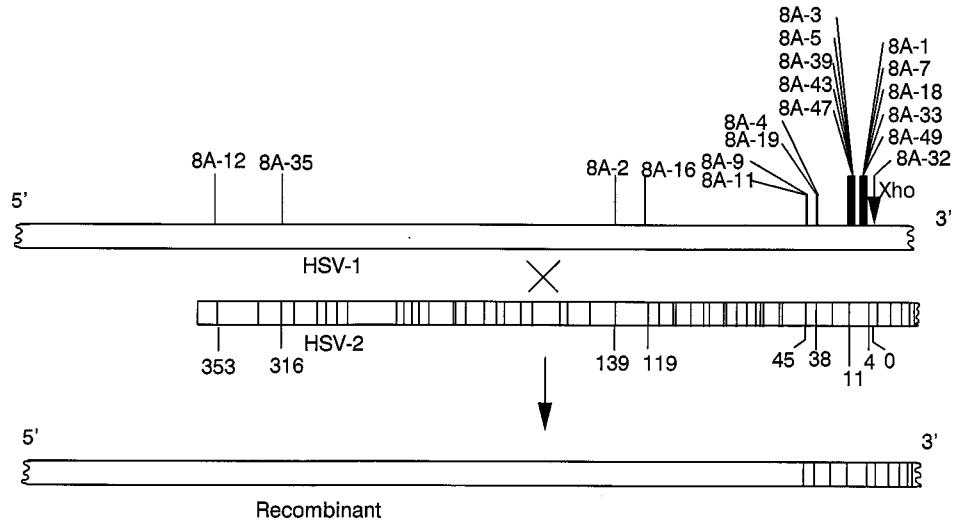

FIG. 10. Intrachromosomal homeologous crossover products in cell line 8A. The top, middle, and bottom illustrations depict parental HSV-1 and HSV-2 *tk* sequences and a particular crossover product, respectively. Only the segment of each *tk* sequence mapping upstream from *Xho*I linker insertion mutation 8 is illustrated. (Top) The positions of the linker insertion (Xho) and crossover sites in hybrid *tk* genes (8A-1, etc.) are indicated. Nineteen independent HAT^r segregants were analyzed. All crossover sites were determined by nucleotide sequencing. Nucleotide differences between HSV-1 and HSV-2 *tk* sequences are represented by vertical lines in the HSV-2 sequence. (Middle) Numbers below the illustration indicate the distances (in base pairs) from the *Xho*I site to various crossover sites. (Bottom) This particular recombinant sequence has a crossover site that is 45 bp from the *Xho*I linker insertion.

bination to start and that the homologous portion of the hybrid donor enhances recombination primarily by providing a site for initiation. For simplicity, we have adopted this latter view as our working hypothesis in much of the following discussion (remaining cognizant that other scenarios haven't been formally ruled out).

With the exception of a single clone, 28N4, from a cell line containing pHYB21-28 (Fig. 4B; Table 2), each gene conversion tract had one terminus mapping within the region of sequence identity between the hybrid donor and the HSV-1 *tk* recipient. The homologous portion of the hybrid donor thus appeared to have enhanced recombination by participating in the initiation (or termination) of actual strand exchange rather than by merely aiding in the initial pairing of sequences. Clone 28N4, in which both conversion tracts end within homeologous sequences, could have arisen by either (i) strand exchange that initiated within homologous sequences and propagated into homeology, forming hDNA that was subject to repair which initiated within homeologous sequences, or (ii) strand exchange that initiated and resolved within homeologous sequences. Although we cannot distinguish between these two possibilities for the genesis of clone 28N4, the first scenario is consistent with our inference that the homologous portion of the hybrid donor stimulated recombination by participating in strand exchange. Conversion tract ends that mapped within homeologous sequences did not appear to be preferentially located within the longest stretches of homology between recipient and donor, with the boundary of tract ends containing as little as 4 bp of sequence identity (Table 2). Similar findings have been reported for homeologous recombination in yeast (15, 18, 32, 34).

For experiments with cell lines containing pHYB521-8, the proposition that both initiation and resolution of recombination occur preferentially within regions of high homology can explain why 24 of 28 recovered events did not display recombination junctions within homeologous *tk* sequences. The observation that all of these 24 events were crossovers rather than gene conversions can be explained by the fact that gene con-

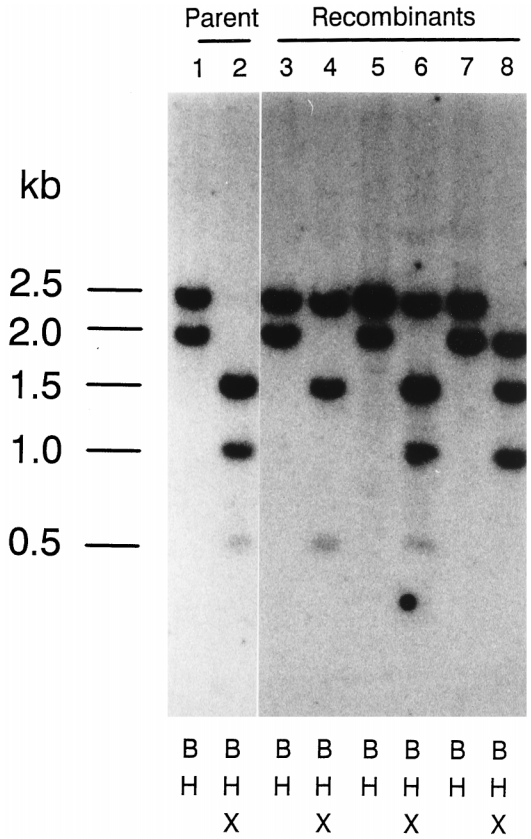

FIG. 11. Southern blotting analysis of cell line JS37 and representative HAT^r recombinants. Genomic DNA (8-μg) samples from parental cell line JS37 (lanes 1 and 2) and three HAT^r segregants (lane 3 through 8) were digested with *Bam*HI plus *Hin*dIII (BH) or *Bam*HI plus *Hin*dIII and *Xho*I (BHX) and displayed in pairs of lanes on a Southern blot with a *tk*-specific probe. The recombinant displayed in lanes 3 and 4 and the recombinant displayed in lanes 7 and 8 exhibit the pattern of hybridizing bands expected for gene conversions of the rightmost and leftmost *tk* genes, respectively (Fig. 12). The pattern of the recombinant displayed in lanes 4 and 5 is consistent with a sister chromatid crossover (Fig. 12). See text for further discussion.

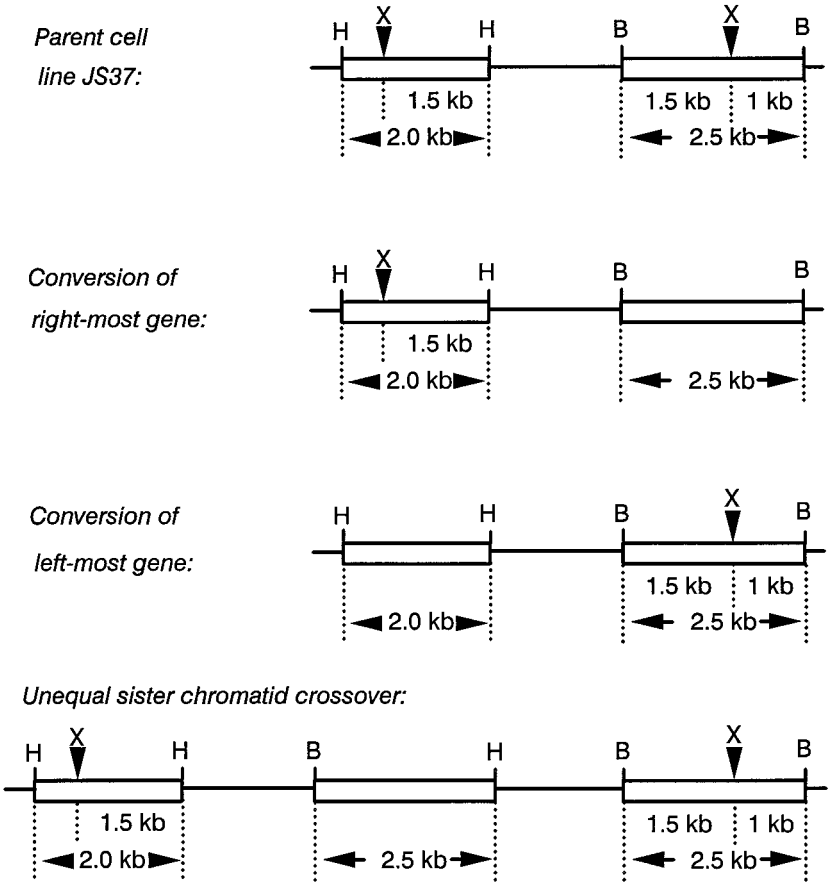

FIG. 12. Structures of construct pJS3 integrated into parental cell line JS37 and three types of HAT^r recombinants. The symbols are the same as those described in the legend to Fig. 1. Indicated for the parental cell line and each type of recombinant are the origins of the expected fragments generated by digestion with *Bam*HI (B), *Hin*dIII (H), and *Xho*I (X) in various combinations and visualized on the Southern blot of Fig. 11.

version tracts beginning and terminating within the 360-bp region of homology downstream from the *Xho*I linker mutation in pHYB521-8 (Fig. 1B) would not have corrected the insertion mutation and would not have been recovered. Interestingly, all four recovered events (recombinants 2a, 4a, 7a, and 10a [Fig. 4A; Table 2]) that did display a recombination junction within homeologous *tk* sequences were gene conversions rather than crossovers. This latter observation indicated that recombination events that traversed homeologous sequences could resolve as gene conversions and that traversing homeology did not appear to promote crossovers. This finding contrasts with the results obtained with cell line 8A and discussed below. The promoter present in the hybrid *tk* sequence on pHYB521-8 (Fig. 1B) did not significantly stimulate the rate of homeologous recombination relative to the rate obtained with pHYB521-8 or pHYB21-28, in which only the HSV-1 *tk* recipient sequence was transcribed. We have similarly found that the rate of intrachromosomal homologous recombination is not elevated when both, rather than only one, of the recombining sequences are actively transcribed (6, 59).

To examine events that both initiated and resolved entirely within homeologous sequences in the absence of any nearby regions of sequence identity, in this and previous works (52, 59), we established a total of 11 independent cell lines derived from mouse L*tk*$^-$ cells containing linked homeologous *tk* sequences. From our collective set of data, we assessed that the overall rate of intrachromosomal homeologous recombination between linked HSV-1 and HSV-2 *tk* genes is $<10^{-9}$ events per cell generation per locus. Mouse cell line 8A is the only cell line tested to date that has reproducibly and unambiguously generated intrachromosomal homeologous recombinants, at a rate of 1.1×10^{-8} events per cell generation per locus (Table 1). This rate is still over 2 orders of magnitude lower than the rate of intrachromosomal homologous recombination measured in the current work with mouse L*tk*$^-$ cell lines containing pJS3 (Fig. 1B) and in previous studies (6, 59). At this time, we do not understand why cell line 8A exhibits an elevated rate of homeologous recombination. (Several of the other 10 cell lines tested had tandem duplications of pTK2TK1-8 as was found in cell line 8A, ruling out the possibility that tandem duplications are solely responsible for the behavior of line 8A.) Cell line 8A represented a singular opportunity to examine pure homeologous recombination within a mammalian genome.

Extensive analyses of intrachromosomal homologous recombination between pairs of direct or inverted repeats of HSV-1 *tk* genes had previously indicated that the majority of intrachromosomal recombination events in mouse L*tk*$^-$ cells are gene conversions without associated crossovers (5, 6, 20, 24, 54). In the current work, experiments with cell lines containing pJS3 (Fig. 1B) provided independent confirmation that gene conversions constitute the most common class (81%) of homologous recombination events recovered. It was therefore striking to find that the majority (20 of 27) of the HAT^r segregants arising from cell line 8A were due to homeologous

crossovers and that none were due to simple gene conversions. These results were also distinctly different from the results obtained with hybrid *tk* donors discussed above, in which homeologous gene conversions were recovered. Equally striking was the observation that 11 of 19 homeologous crossover sites were clustered within 11 bp and that 15 of 19 crossover sites were clustered within 45 bp of the position of the *Xho*I linker insertion in the HSV-1 *tk* gene (Fig. 10; Table 3). Theoretically, a crossover anywhere within the 367-bp interval between the 5′ end of the HSV-2 *tk* sequence and the position of the *Xho*I linker insertion 8 in the HSV-1 *tk* gene (Fig. 5) would have produced a functional *tk* gene. Studies of recombinant *tk* genes generated extrachromosomally indeed revealed that many different types of proteins encoded by hybrid HSV-1–HSV-2 *tk* genes are functional (52, 59). The clustered crossover sites also did not correspond to the longest available regions of sequence identity (Fig. 5; Table 3). How may we reconcile our various observations?

Our results suggest that the types of recombination events which occur in a mammalian genome are critically influenced by the degree of sequence divergence at the site of recombination initiation. Similar inferences have recently been made for recombination in yeast (12, 34). We infer that the hybrid donor sequences of our recombination substrates provided an amount of homology sufficient for the initiation of events that are mechanistically analogous to perfectly homologous crosses. We envision that the amount of homology needed for the initiation of such events is equal to the minimal efficient processing segment (MEPS) (44), which we previously estimated to be >130 bp of sequence identity for mammalian cells (53). Adjoining homeology appears to pose somewhat of a barrier for recombination that initiates within MEPS, as illustrated in particular by the results of experiments with pHYB521-8 described above as well as the relatively low recombination rates observed for constructs pHYB521-8 and pHYB21-28 (about 10-fold lower overall than the rate of recombination between homologous sequences with 360 bp of perfect homology, the length of the homologous segment on each hybrid donor [53, 59]). This barrier, which is not entirely impenetrable, may be due to a heteroduplex rejection mechanism regulated by DNA mismatch repair machinery, as previously described for yeast (1, 12, 43) and bacteria (39, 57).

When homology in excess of MEPS is not available, we reason that the usual mechanism for homologous recombination cannot be initiated and therefore the recombination rate is drastically reduced. Such was the case in experiments that involved purely homeologous crosses between HSV-1 and HSV-2 *tk* sequences. We consider it an important observation that among a total of 11 different cell lines studied in this and earlier works (52, 59), which collectively included 27 integrated copies of pTK2TK1-8, we have never recovered a homeologous gene conversion which corrected the *Xho*I linker insertion mutation contained in our substrate. Indeed, in the one cell line, 8A, from which we have recovered homeologous recombination events, each of the unambiguous homeologous recombination events was a crossover. Our findings thus indicate that for the exceptional cell line in which homeologous sequences did recombine, the pathway employed was different from that normally used for homologous recombination.

The marked clustering of crossover junctions near the *Xho*I linker in cell line 8A might originate from any of several mechanisms. One possibility is that highly mismatched hDNA which also contained an insertion loop heterology (which would be produced if the hDNA encompassed the linker insertion) was efficiently targeted and destroyed by mismatch repair machinery. Alternatively, branch migration that initiated within homeologous sequences may not have been able to pass through an insertion-type heterology. In either of these scenarios, hDNA that encompassed the linker insertion would be effectively disallowed and thus the insertion mutation would not be correctable via gene conversion. (Conversion via double-strand gap repair was also clearly not an operative pathway.) These scenarios explain the lack of gene conversions but do not readily explain the clustering of crossover sites close to the linker insertion. A different possibility is that the *Xho*I linker insertion, which is palindromic in nature (the sequence of the insert is CCTCGAGGCCTCGAGG), is particularly susceptible to cleavage and that it served as an initiation site of recombination with limited branch migration. Perhaps strand breakage at or near the palindrome induced single-strand annealing events. An attractive hypothesis is that homeologous crossovers in cell line 8A were generated during DNA replication by template switching that occurred preferentially in close proximity to the palindromic *Xho*I linker insertion. We present a model (Fig. 13), based in part on a recently described model for homeologous recombination in yeast (34, 35), in which the 3′ end of a nascent DNA strand invades a homeologous sequence and is extended by replication with the homeologous sequence as the template. This type of mechanism bears similarities to templated end extensions of transfected DNA molecules seen in gene targeting (42), as well as the "copy-join" process recently proposed for illegitimate integration of DNA into mammalian cells (29). In light of the proposed replication-slippage model, the unusual ability of cell line 8A to produce homeologous recombinants may be related to the sites of integration of pTK2TK1-8 with regard to genomic replication origins.

A one-sided invasion model has been presented by others (3) for homeologous or homologous recombination between exogenous and endogenous LINE-1 sequences in mouse cells. Similar to our proposed replication-slippage model for intrachromosomal homeologous recombination in cell line 8A, re-

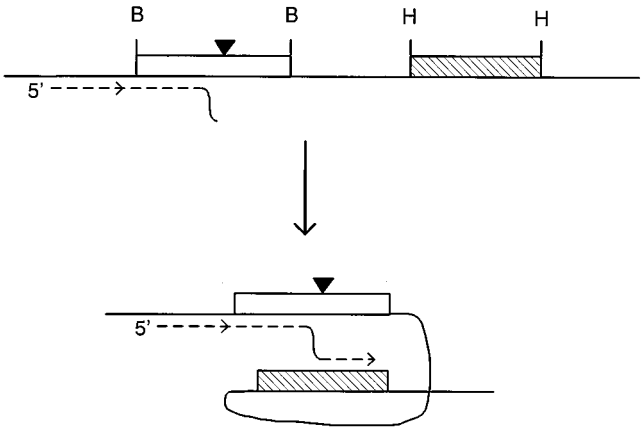

FIG. 13. Replication slippage mechanism for homeologous crossover in cell line 8A. In this simplified illustration, newly synthesized DNA is indicated by a broken line. The remaining symbols are the same as those described in the legend to Fig. 1, except that the template for DNA replication is understood to be single stranded. DNA replication proceeds up to the *Xho*I linker insertion mutation in the HSV-1 *tk* gene, where the secondary structure of the palindromic insertion brings about a pause of DNA polymerase. Template switching then ensues as the 3′ end of the nascent DNA strand invades the nearby homeologous HSV-2 *tk* gene sequence. This invasion likely involves the pairing of the nascent 3′ end to a short stretch of homology in the HSV-2 *tk* sequence. DNA synthesis resumes with the HSV-2 *tk* sequence as the template, forming a stable intermediate comprised mostly of homoduplex DNA. Such template switching could ultimately produce a homeologous crossover. (Additional steps not depicted would be necessary to resolve the event.).

combination was envisioned as proceeding via invasion by a 3′ DNA end followed by extension of this DNA end with a homeologous or homologous template. In that study (3), the invading 3′ end was provided by linearization of an exogenous substrate by restriction digestions prior to transfection. In our proposal for intrachromosomal homeologous recombination (Fig. 13), the active 3′ end is provided in vivo by replication pausing-slippage.

Our proposed replication template switching model is supported by several observations made by others. Inverted repeats have been shown to be sites of genomic instability in yeast (17), and this instability appears to be mediated through DNA polymerase slippage when the polymerase encounters the base of a stem-loop structure that may be formed by an inverted repeat. Evidence (reviewed in reference 55) that a stem-loop structure in a DNA template may serve as a replication pause site which induces crossovers by template switching has also previously been presented. There have been reports of viral RNA-RNA recombination that occurs preferentially at the base of hairpin structures by a replicase-mediated copy choice mechanism (11). Slipped mispairing during DNA replication has also been discussed as a mechanism for generating deletions between short direct repeats in the human genome (8). Finally, RecA-independent crossovers that proceed via a replication slippage mechanism have been observed in *Escherichia coli* (25).

A salient feature of our model (Fig. 13) and the yeast model for homeologous recombination (34, 35) is that homeologous recombination proceeds without the need for branch migration through highly mismatched sequences. Replication from the invading 3′ end produces a stable recombination intermediate composed mostly of homoduplex DNA. Since the processing of or blockage of formation of a highly mismatched hDNA intermediate by mismatch repair proteins may present a barrier to recombination between diverged sequences in mammals (14), as has been demonstrated for yeast and bacteria (1, 12, 39, 43, 57), template switching during replication can potentially provide a pathway for accomplishing homeologous recombination by effectively evading the cellular mismatch repair machinery.

A potentially testable hypothesis is that homeologous recombination involving hybrid donor sequences, which presumably proceeds through the formation of a highly mismatched hDNA intermediate initiating within a region of sequence identity, is regulated by mammalian mismatch repair functions but that purely homeologous recombination is not. Of particular relevance to this issue are recent studies of yeast (12, 34) which have revealed that recombination between moderately (9%) diverged sequences is regulated by mismatch repair machinery but that recombination between more highly (23 or 14%) diverged sequences is not. Those authors conjecture, as do we for mammalian cells, that the regulation of recombination is critically related to whether the degree of homology available is sufficient for normal initiation of homologous recombination. To further dissect the molecular mechanisms of regulation of genetic recombination in mammalian cells, comparative analyses of homologous and homeologous recombination in mammalian cells with alterations in mismatch repair and/or DNA replication should be of great value.

ACKNOWLEDGMENTS

This work was supported by Public Health Service grant GM47110 from the National Institute of General Medical Sciences to A.S.W.

We thank Barbara Criscuolo Waldman for helpful comments.

REFERENCES

1. **Alani, E., R. A. G. Reenan, and R. D. Kolodner.** 1994. Interaction between mismatch repair and genetic recombination in *Saccharomyces cerevisiae*. Genetics **137:**19–39.
2. **Bailis, A. M., and R. Rothstein.** 1990. A defect in mismatch repair in *Saccharomyces cerevisiae* stimulates ectopic recombination between homeologous genes by an excision repair dependent process. Genetics **126:**535–547.
3. **Belmaaza, A., E. Milot, J.-F. Villemure, and P. Chartrand.** 1994. Interference of DNA sequence divergence with precise recombinational DNA repair in mammalian cells. EMBO J. **13:**5355–5360.
4. **Bollag, R. J., D. R. Elwood, E. D. Tobin, A. R. Godwin, and R. M. Liskay.** 1992. Formation of heteroduplex DNA during mammalian intrachromosomal gene conversion. Mol. Cell. Biol. **12:**1546–1552.
5. **Bollag, R. J., and R. M. Liskay.** 1988. Conservative intrachromosomal recombination between inverted repeats in mouse cells: association between reciprocal exchange and gene conversion. Genetics **119:**161–169.
6. **Bollag, R. J., A. S. Waldman, and R. M. Liskay.** 1989. Homologous recombination in mammalian cells. Annu. Rev. Genet. **23:**199–225.
7. **Brinster, R. L., R. E. Braun, D. Lo, M. R. Avarbock, F. Oram, and R. Palmiter.** 1989. Targeted correction of a major histocompatibility class II E^{α} gene by DNA microinjected into mouse eggs. Proc. Natl. Acad. Sci. USA **86:**7087–7091.
8. **Canning, S., and T. P. Dryja.** 1989. Short, direct repeats at the breakpoints of deletions of the retinoblastoma gene. Proc. Natl. Acad. Sci. USA **86:**5044–5048.
9. **Capecchi, M. S.** 1980. High efficiency transformation by direct microinjection of DNA into cultured mammalian cells. Cell **22:**479–488.
10. **Capizzi, R. L., and J. W. Jameson.** 1973. A table for the estimation of the spontaneous mutation rate of cells in culture. Mutat. Res. **17:**147–148.
11. **Carpenter, C. D., J. W. Oh, C. Zhang, and A. E. Simon.** 1995. Involvement of a stem-loop structure in the location of junction sites in viral RNA recombination. J. Mol. Biol. **245:**608–622.
12. **Datta, A., A. Adjiri, L. New, G. Crouse, and S. Jinks-Robertson.** 1996. Mitotic crossovers between diverged sequences are regulated by mismatch repair proteins in *Saccharomyces cerevisiae*. Mol. Cell. Biol. **16:**1085–1093.
13. **Desautels, L., S. Brouillette, J. Wallenburg, A. Belmaaza, N. Gusew, P. Trudel, and P. Chartrand.** 1990. Characterization of nonconservative homologous junctions in mammalian cells. Mol. Cell. Biol. **10:**6613–6618.
14. **de Wind, N., M. Dekker, A. Berns, M. Radman, and H. te Riele.** 1995. Inactivation of the mouse *Msh2* gene results in mismatch repair deficiency, methylation tolerance, hyperrecombination, and predisposition to cancer. Cell **82:**321–330.
15. **Ernst, J. F., J. W. Stewart, and F. Sherman.** 1981. The *cyc1-11* mutation in yeast reverts by recombination with a non-allelic gene: composite genes determining the isocytochromes c. Proc. Natl. Acad. Sci. USA **78:**6334–6338.
16. **Goguel, V., A. Delahodde, and C. Jacq.** 1992. Connections between RNA splicing and DNA intron mobility in yeast mitochondria: RNA maturase and DNA endonuclease switching experiments. Mol. Cell. Biol. **12:**696–705.
17. **Gordenin, D. A., K. S. Lobachev, N. P. Degtyareva, A. L. Malkova, E. Perkins, and M. A. Resnick.** 1993. Inverted DNA repeats: a source of eukaryotic genomic instability. Mol. Cell. Biol. **13:**5315–5322.
18. **Harris, S., K. S. Rudnicki, and J. E. Haber.** 1993. Gene conversions and crossing over during homologous and homeologous ectopic recombination in *Saccharomyces cerevisiae*. Genetics **135:**5–16.
19. **Kit, S., M. Kit, H. Qavi, D. Trkula, and H. Otsuka.** 1983. Nucleotide sequence of the herpes simplex virus type 2 (HSV-2) thymidine kinase gene and predicted amino acid sequence of thymidine kinase polypeptide and its comparison with the HSV-1 thymidine kinase gene. Biochim. Biophys. Acta **741:**158–170.
20. **Letsou, A., and R. M. Liskay.** 1986. Intrachromosomal recombination in mammalian cells, p. 383–409. *In* R. Kucherlapati (ed.), Gene transfer. Plenum, New York, N.Y.
21. **Letsou, A., and R. M. Liskay.** 1987. Effect of the molecular nature of mutation on the efficiency of intrachromosomal gene conversion in mouse cells. Genetics **117:**759–769.
22. **Liskay, R. M., A. Letsou, and J. L. Stachelek.** 1987. Homology requirement for efficient gene conversion between duplicated chromosomal sequences in mammalian cells. Genetics **115:**161–167.
23. **Liskay, R. M., and J. L. Stachelek.** 1986. Information transfer between duplicated chromosomal sequences in mammalian cells involves contiguous regions of DNA. Proc. Natl. Acad. Sci. USA **83:**1802–1806.
24. **Liskay, R. M., J. L. Stachelek, and A. Letsou.** 1984. Homologous recombination between repeated chromosomal sequences in mouse cells. Cold Spring Harbor Symp. Quant. Biol. **49:**183–189.
25. **Lovett, S. T., P. T. Drapkin, V. A. Sutera, Jr., and T. J. Gluckman-Peskind.** 1993. A sister-chromatid exchange mechanism for recA-independent deletion of repeated DNA sequences in *Escherichia coli*. Genetics **135:**631–642.
26. **Lukacsovich, T., D. Yang, and A. S. Waldman.** 1994. Repair of a specific double-strand break generated within a mammalian chromosome by yeast endonuclease I-*Sce*I. Nucleic Acids Res. **22:**5649–5657.
27. **Luria, S. F., and M. Delbrück.** 1943. Mutations of bacteria from virus sensitivity to virus resistance. Genetics **28:**491–511.

28. **Matic, I., M. Radman, and C. Rayssiguier.** 1994. Structure of recombinants from conjugational crosses between *Escherichia coli* donor and mismatch-repair deficient *Salmonella typhimurium* recipients. Genetics **136:**17–26.
29. **Merrihew, R. V., K. Marburger, S. L. Pennington, D. B. Roth, and J. H. Wilson.** 1996. High-frequency illegitimate integration of transfected DNA at preintegrated target sites in a mammalian genome. Mol. Cell. Biol. **16:**10–18.
30. **Meselson, M. S., and C. M. Radding.** 1975. A general model for genetic recombination. Proc. Natl. Acad. Sci. USA **72:**358–361.
31. **Mézard, C., and A. Nicolas.** 1994. Homologous, homeologous, and illegitimate repair of double-strand breaks during transformation of a wild-type and a *rad52* mutant strain of *Saccharomyces cerevisiae*. Mol. Cell. Biol. **14:**1278–1292.
32. **Mézard, C., D. Pompon, and A. Nicolas.** 1992. Recombination between similar but not identical DNA sequences during yeast transformation occurs within short stretches of identity. Cell **70:**659–670.
33. **Petes, T. D., R. E. Malone, and L. S. Symington.** 1991. Recombination in yeast, p. 407–521. *In* J. R. Broach, J. R. Pringle, and E. W. Jones (ed.), The molecular and cellular biology of the yeast *Saccharomyces*: genome dynamics, protein synthesis, and energetics. Cold Spring Harbor Laboratory Press, Plainview, N.Y.
34. **Porter, G., J. Westmoreland, S. Priebe, and M. A. Resnick.** 1996. Homologous and homeologous intermolecular gene conversions are not differently affected by mutations in the DNA damage or the mismatch repair genes *RAD1*, *RAD50*, *RAD51*, *RAD52*, *RAD54*, *PMS1*, and *MSH2*. Genetics **143:** 755–767.
35. **Priebe, S. D., J. Westmoreland, T. Nilsson-Tillgren, and M. A. Resnick.** 1994. Induction of recombination between homologous and diverged DNAs by double-strand gaps and breaks and role of mismatch repair. Mol. Cell. Biol. **14:**4802–4814.
36. **Radman, M.** 1988. Mismatch repair and genetic recombination, p. 169–192. *In* R. Kucherlapati and G. R. Smith (ed.), Genetic recombination. American Society for Microbiology, Washington, D.C.
37. **Radman, M.** 1989. Mismatch repair and the fidelity of genetic recombination. Genome **31:**68–73.
38. **Rayssiguier, C., C. Dohet, and M. Radman.** 1991. Interspecific recombination between *Escherichia coli* and *Salmonella typhimurium* occurs by the RecABCD pathway. Biochimie **73:**371–374.
39. **Rayssiguier, C., D. S. Thaler, and M. Radman.** 1989. The barrier to recombination between *Escherichia coli* and *Salmonella typhimurium* is disrupted in mismatch-repair mutants. Nature **342:**396–401.
40. **Resnick, M. A., Z. Zgaga, P. Hieter, J. Westmoreland, S. Fogel, and T. Nilsson-Tillgren.** 1992. Recombinational repair of diverged DNAs: a study of homeologous chromosomes and mammalian YACs in yeast. Mol. Gen. Genet. **234:**65–73.
41. **Rubnitz, J., and S. Subramani.** 1984. The minimum amount of homology required for homologous recombination in mammalian cells. Mol. Cell. Biol. **4:**2253–2258.
42. **Scheerer, J. B., and G. M. Adair.** 1994. Homology dependence of targeted recombination at the Chinese hamster *APRT* locus. Mol. Cell. Biol. **14:**6663–6673.
43. **Selva, E. M., L. New, G. F. Crouse, and R. S. Lahue.** 1995. Mismatch correction acts as a barrier to homeologous recombination in *Saccharomyces cerevisiae*. Genetics **139:**1175–1188.
44. **Shen, P., and H. V. Huang.** 1986. Homologous recombination in *Escherichia coli*: dependence on substrate length and homology. Genetics **112:**441–457.
45. **Shen, P., and H. V. Huang.** 1989. Effect of base pair mismatches on recombination via the RecBCD pathway. Mol. Gen. Genet. **218:**358–360.
46. **Southern, P. S., and P. Berg.** 1982. Transformation of mammalian cells to antibiotic resistance with a bacterial gene under control of the SV40 early promoter. J. Mol. Appl. Genet. **1:**327–341.
47. **Stachelek, J., and R. M. Liskay.** 1988. Accuracy of intrachromosomal gene conversion in mouse cells. Nucleic Acids Res. **16:**4069–4076.
48. **Subramani, S., and B. L. Seaton.** 1988. Homologous recombination in mitotically dividing mammalian cells, p. 549–573. *In* R. Kucherlapati and G. R. Smith (ed.), Genetic recombination. American Society for Microbiology, Washington, D.C.
49. **Swain, M. A., and D. A. Galloway.** 1983. Nucleotide sequence of the herpes simplex virus type 2 thymidine kinase gene. J. Virol. **46:**1045–1050.
50. **Szostak, J. W., T. L. Orr-Weaver, R. J. Rothstein, and F. W. Stahl.** 1983. The double-strand break repair model for recombination. Cell **33:**25–35.
51. **Wagner, M. J., J. A. Sharp, and W. C. Summers.** 1981. Nucleotide sequence of the thymidine kinase gene of herpes simplex virus type 1. Proc. Natl. Acad. Sci. USA **78:**1441–1445.
52. **Waldman, A. S., and R. M. Liskay.** 1987. Differential effects of base-pair mismatch on intrachromosomal versus extrachromosomal recombination in mouse cells. Proc. Natl. Acad. Sci. USA **84:**5340–5344.
53. **Waldman, A. S., and R. M. Liskay.** 1988. Dependence of intrachromosomal recombination in mammalian cells on uninterrupted homology. Mol. Cell. Biol. **8:**5350–5357.
54. **Waldman, A. S., and B. C. Waldman.** 1991. Stimulation of intrachromosomal homologous recombination in mammalian cells by an inhibitor of poly(ADP-ribosylation). Nucleic Acids Res. **19:**5943–5947.
55. **Wells, R. D.** 1996. Molecular basis of genetic instability of triplet repeats. J. Biol. Chem. **271:**2875–2878.
56. **Wheeler, C. J., D. Maloney, S. Fogel, and R. S. Goodenow.** 1990. Microconversion between murine H-2 genes integrated into yeast. Nature **347:**192–194.
57. **Worth, L., S. Clark, M. Radman, and P. Modrich.** 1994. Mismatch repair proteins MutS and MutL inhibit RecA-catalyzed strand transfer between diverged DNAs. Proc. Natl. Acad. Sci. USA **91:**3238–3241.
58. **Yang, D., and A. S. Waldman.** 1992. An examination of the effects of double-strand breaks on extrachromosomal recombination in mammalian cells. Genetics **132:**1081–1093.
59. **Yang, D., and A. S. Waldman.** Unpublished data.